Journal of Pharmaceutical and Biomedical Analysis 140 (2017) 113–121

Contents lists available at ScienceDirect

Journal of Pharmaceutical and Biomedical Analysis

journal homepage: www.elsevier.com/locate/jpba

Heparin and homogeneous model heparin oligosaccharides form distinct complexes with protamine: Light scattering and zeta potential analysis

Cynthia D. Sommers[a,*], Hongping Ye[a], Jian Liu[b], Robert J. Linhardt[c], David A. Keire[a]

[a] Food and Drug Administration, CDER, Division of Pharmaceutical Analysis, 63110 St Louis, MO, USA
[b] Division of Chemical Biology and Medicinal Chemistry, Eshelman School of Pharmacy, University of North Carolina, 27599 Chapel Hill, NC, USA
[c] Department of Chemistry and Chemical Biology, Center for Biotechnology and Interdisciplinary Studies, Rensselaer Polytechnic Institute, Troy, NY, USA

ARTICLE INFO

Article history:
Received 30 December 2016
Received in revised form 6 February 2017
Accepted 9 March 2017
Available online 14 March 2017

Keywords:
Heparin
Protamine
Complex
Heparin induced thrombocytopenia (HIT)
dynamic light scattering
Zeta (ξ) potential

ABSTRACT

Large multimolecular complexes of heparin with positively charged proteins such as platelet factor 4 (PF4) or protamine can initiate immune responses associated with heparin use in patients, including the most significant adverse event, heparin-induced thrombocytopenia (HIT). Current evidence suggests that platelet-activating antibodies that recognize large multi-molecular complexes (300–700 kDa) of PF4 bound to heparin cause HIT [1] and in very rare cases anti-protamine-heparin antibodies can induce thrombocytopenia [2]. Heparin is administered as a mixture of sulfated glycosaminoglycans of variable lengths and sulfation levels. To date the potential impact of chain length, sulfation level and impurities on the formation, size and immunogenicity of heparin-protamine complexes has not been addressed due to the lack of purified, homogenous heparin chains for testing purposes. Here, a set of well-characterized model heparin oligosaccharides was used with protamine sulfate to evaluate the physicochemical properties of the resulting complexes. Hydrodynamic radii and zeta potential profiles of heparin-protamine complexes were observed to be dependent upon the sulfation location, size and concentration of the model heparin oligosaccharides. The well-characterized oligosaccharide-protamine complexes analyzed in this work will be useful for establishing links between heparin-protamine complex physiochemical attributes to their potential to illicit cellular immunogenicity.

Published by Elsevier B.V.

1. Introduction

Evaluation of potential immunogenicity or immune reactivity is a significant challenge in the development of new biotherapeutics [3]. Currently, the most frequent immune-mediated adverse drug reaction affecting blood cells is induced by the commonly used anticoagulant heparin [4]. Heparin, a highly charged polyanion, has the propensity to bind and form immunogenic complexes (300–700 kDa) with platelet factor 4 (PF4). Heparin consists of disaccharide repeating units of →4) D-GlcA β(1→4) D-GlcN α(1→ and →4) L-IdoA α(1→4)D-GlcN α(1→, where D-GlcA represents D-glucuronic acid, L-IdoA represents L-iduronic acid, and D-GlcN represents D-glucosamine. Each sugar residue can carry *O*-sulfo groups and the GlcN can also carry *N*-sulfo or *N*-acetyl groups, resulting in a mixture of sulfated molecules with a range of chain lengths and molecular weights from 8000 to 40,000 Da [5,6]. Antibodies to H-PF4 can then trigger heparin-induced thrombocytopenia (HIT) and thrombosis [1,4].

Currently, there is no clear understanding of the factors that impact the immunogenicity of heparin and trigger disease. However, low molecular weight heparins (LMWH) are known to have reduced the risk of HIT, which suggests that heparin chain length is a factor in the pathogenesis of HIT. Unfortunately, LMWH, formed through heparin depolymerization, still contain a heterogeneous mixture of polysaccharides with molecular weights ranging from 3500 to 6000 Da [7,8]. Recent studies using synthetic oligosaccharides provide evidence that "heparin-like" molecules can be developed with anti-coagulant, anti-thrombotic and in vivo hemorrhagic activities similar to heparin or LMWH with sufficient reversibility to protamine [9,10]. However, these studies did not

* Corresponding author at: FDA/DPA, 645 S. Newstead Ave., St. Louis, MO, 63110, Tel.: +314 539 2177.
E-mail address: Cynthia.Sommers@fda.hhs.gov (C.D. Sommers).

http://dx.doi.org/10.1016/j.jpba.2017.03.010
0731-7085/Published by Elsevier B.V.

Table 1
Structural information of model heparin oligosaccharides.

Standard name	Size	# of sulfo groups	IdoA2S	Expected MW Da	Proposed structures
N-acetyl 10-mer	10-mer	0	Without	2036	GlcNAc-(GlcA-GlcNAc)$_4$-GlcA-pNP
NS 10-mer	10-mer	5	Without	2226	GlcNS-(GlcA-GlcNS)$_4$-GlcA-pNP
NS6S 10-mer	10-mer	10	Without	2626	GlcNS6S-(GlcA-GlcNS6S)$_4$-GlcA-pNP
NS2S 10-mer	10-mer	7	With	2428	GlcNAc-GlcA-GlcNS-(IdoA2S-GlcNS)$_3$-GlcA-pNP
NS6S2S 10-mer	10-mer	12	With	2828	GlcNAc6S-GlcA-GlcNS6S-(IdoA2S-GlcNS6S)$_3$-GlcA-pNP
N-acetyl 12-mer	12-mer	0	Without	2415	GlcNAc-(GlcA-GlcNAc)$_5$-GlcA-pNP
NS 12-mer	12-mer	6	Without	2643	GlcNS-(GlcA-GlcNS)$_5$-GlcA-pNP
NS6S 12-mer	12-mer	12	Without	3124	GlcNS6S-(GlcA-GlcNS6S)$_5$-GlcA-pNP
NS2S 12-mer	12-mer	9	With	2925	GlcNAc-GlcA-GlcNS-(IdoA2S-GlcNS)$_4$-GlcA-pNP
NS2S6S 12-mer	12-mer	15	With	3406	GlcNAc6S-GlcA-GlcNS6S-(IdoA2S-GlcNS6S)$_4$-GlcA-pNP
N-acetyl 14-mer	14-mer	0	Without	2794	GlcNAc-(GlcA-GlcNAc)$_6$-GlcA-pNP
NS 14-mer	14-mer	7	Without	3061	GlcNS-(GlcA-GlcNS)$_6$-GlcA-pNP
NS6S 14-mer	14-mer	14	Without	3621	GlcNS6S-(GlcA-GlcNS6S)$_6$-GlcA-pNP
NS2S 14-mer	14-mer	12	With	3461	GlcNS-GlcA-GlcNS-(IdoA2S-GlcNS)$_5$-GlcA-pNP
NS6S2S 14-mer	14-mer	19	With	4021	GlcNS6S-GlcA-GlcNS6S-(IdoA2S-GlcNS6S)$_5$-GlcA-pNP
N-acetyl 16-mer	16-mer	0	Without	3174	GlcNAc-(GlcA-GlcNAc)$_7$-GlcA-pNP
NS 16-mer	16-mer	8	Without	3478	GlcNS-(GlcA-GlcNS)$_7$-GlcA-pNP
NS6S 16-mer	16-mer	16	Without	4118	GlcNS6S-(GlcA-GlcNS6S)$_7$-GlcA-pNP
NS2S 16-mer	16-mer	14	With	3958	GlcNS-GlcA-GlcNS-(IdoA2S-GlcNS)$_6$-GlcA-pNP
NS6S2S 16-mer	16-mer	22	With	4599	GlcNS6S-GlcA-GlcNS6S-(IdoA2S-GlcNS6S)$_6$-GlcA-pNP
N-acetyl 18-mer	18-mer	0	Without	3553	GlcNAc-(GlcA-GlcNAc)$_8$-GlcA-pNP
NS 18-mer	18-mer	9	Without	3897	GlcNS-(GlcA-GlcNS)$_8$-GlcA-pNP
NS6S 18-mer	18-mer	18	Without	4616	GlcNS6S-(GlcA-GlcNS6S)$_8$-GlcA-pNP
NS2S 18-mer	18-mer	16	With	4456	GlcNS-GlcA-GlcNS-(IdoA2S-GlcNS)$_7$-GlcA-pNP
NS6S2S 18-mer	18-mer	25	With	5176	GlcNS6S-GlcA-GlcNS6S-(IdoA2S-GlcNS6S)$_7$-GlcA-pNP

address potential immunogenic responses or evaluate the physicochemical properties of complexes formed by these analogs.

Protamine sulfate is clinically used as an antidote of heparin and forms ultra-large immunogenic complexes with heparin that bear similarities with immune complexes of PF4 and heparin. For example, these complexes are immunogenic in mice and result in the formation of antibodies, which activate platelets in cardiopulmonary bypass surgery patients and have caused thrombocytopenia in rare instances [2,11–13]. Therefore, protamine represents a clinically relevant and less expensive reagent than PF4 to characterize analytical models used to assess risks associated with heparin/protein complexes.

Assembly of protamine-heparin complexes is influenced by small changes in the stoichiometric ratios of protamine and heparin [7,11]. These interactions display colloidal properties, where negatively charged heparin neutralizes the positive charges on protamine to facilitate the formation of immunogenic ultra-large complexes at neutral pH [11]. As expected of colloidal interactions, complex sizes are maximal when the net surface charge of complexes is neutralized. When heparin or its binding proteins are in excess, the complex is destabilized through forces of charge repulsion. Studies show that sensitization in vivo is highly dependent upon the net surface charge of heparin protein complexes as well as their actual size [11,14]. Furthermore, the point of complex surface charge neutrality and formation of ultra large forms (as measured by light scattering) are correlated with in vitro and in vivo measures of immunogenicity [14].

Therefore, the use of methods to assess complex size and surface charge of heparin protamine complexes was investigated. For example, zeta (ξ) potential, a measurement of net surface charge, can be used to determine optimal stoichiometry of reactants to reach neutrality (i.e., the point at which the ξ potential value is 0). The formation of ultra large complexes can also be tracked by changes in light absorption at 280 nm (turbidity) or the actual size can be confirmed by dynamic light scattering (DLS, also known as photon correlation spectroscopy, PCS, and quasi-elastic light scattering, QELS), microscopy or sedimentation velocity [11,14,15].

To date, studies to assess the impact of chain length and sulfation patterns on the formation and size of heparin antibody complexes and anti-coagulation activities have been hampered by the absence of well-defined homogeneous heparin oligosaccharides. The studies herein characterize the formation of heparin-protamine complexes using a set of characterized model heparin oligosaccharides, differing in size and charge, using models of ξ potential and DLS.

2. Materials and Methods

2.1. Materials

Heparin (USP 1304038; MW ~15,600 [16]), Enoxaparin (USP 1235820; MW ~ 3900 Da [16]) and protamine sulfate (Sigma P3369, MW ~5000 Da) were supplied by Sigma (St. Louis, MO). Model heparin oligosaccharides of different sequences and lengths, including 10, 12, 14, 16 and 18-mers, were synthesized and characterized by Professors Jian Liu (University of North Carolina) and Robert Linhardt (Rensselaer Polytechnic Institute).

2.2. Synthesis of Model Heparin Oligosaccharides

The oligosaccharides were synthesized using a chemoenzymatic approach starting from a monosaccharide with a structure of GlcA-pNP (GlcA, represents glucuronic acid; pNP represents *p*-nitrophenyl). The detailed procedures for the synthesis are described in previous publications [17,18]. The HPLC analyses were carried out using a DEAE-NPR column (Tosoh Biosciences, King of Prussia, PA) or using a silica-based polyamine (PAMN) HPLC column (Waters, Milford, MA).

2.3. Characterization of Model Heparin Oligosaccharides

2.3.1. MS Analysis

The low-resolution analyses were performed on a Thermo LCQ-Deca. The MS data were acquired and processed using Xcalibur 1.3. High resolution ESI-MS analysis was conducted on Thermo LTQ XL Orbitrap (Bremen, Germany). A Luna hydrophilic liquid interaction chromatography (HILIC) column (2.0 × 150 mm^2, 200 Å, Phenomenex, Torrance, CA) was used to separate the oligosaccharide mixture. The LC column was directly connected online to the standard electrospray ionization source of LTQ-Orbitrap XL Fourier

Table 2
Summary of intercepts and peak values of 12-mers complexed with protamine[t] from analytical models.

Heparin	X axis intercept zeta potential	Radius (nm) ratio 1.7	Peak ratio OD280	Peak OD280 (nm)
Hep	1.44	51 (0.8)	1.35	1.20
Enox	1.40	48 (0.4)	0.90	1.01
12-NS6S2S	1.40	51 (0.4)	1.35	0.67
12-NS6S	1.09	66 (0.2)*	1.35	0.66
12-NS2S	1.15	262 (4.4)**	1.35	0.68
12-NS	0.95	265 (8.1)**	0.90	0.66

[t] Average ± standard deviation radii of protamine alone 18.3 (5.6) nm.
* $t < 0.001$.
** $t < 0.0001$ 2 tailed-t test comparison of radii at 3 min versus 60 min.

transform (FT) mass spectrometer (MS) (Thermo Fisher Scientific, San-Jose, CA). All FT mass spectra were acquired at a resolution of 60,000 with 300 – 2000 Da mass range.

2.3.2. NMR Analysis

All model heparin oligosaccharides were analyzed by 1D ^{1}H-NMR, 1D ^{13}C-NMR and 2D NMR (^{1}H–^{1}H COSY, ^{1}H–^{13}C HSQC) on Varian Inova 500 MHz spectrometer with VnmrJ 2.2D software. Samples (2.0–5.0 mg) were dissolved in 0.5 mL D_2O (99.994%, Sigma-Aldrich) and lyophilized three times to remove the exchangeable protons. The samples were re-dissolved in 0.5 mL D_2O and transferred to NMR microtubes (OD 5 mm, Norrell). 1D ^{1}H-NMR experiments were performed with 256 scans and an acquisition time of 768 ms. 1D ^{13}C-NMR experiments were performed with 40,000 scans, 1.0 s relaxation delay, and an acquisition time of 1000 ms. 2D ^{1}H–^{1}H COSY experiments were performed with 48 scans, 1.8 s relaxation delay, and 204 ms acquisition time. 2D ^{1}H–^{13}C HSQC experiments were performed with 48 scans, 1.5 s relaxation delay, and 256 ms acquisition time (Table 1).

2.4. Zeta Potential and Hydrodynamic Radius

Samples were prepared by mixing equal parts of filtered (0.1 μm) 2x protamine (0.2 mg/mL) and heparin/oligosaccharide (0.2–0.05 mg/mL) stock solutions (Milli-Q water). A Protamine-oligosaccharide ratio of 1.7 was used for data shown in Tables 2 and 3 and in Fig. 4. Sample (65 μL) was placed in a flow cell and read at room temperature using a Mobius®, a light scattering instrument (Wyatt, Santa Barbara, CA). The zeta potential method was based on a measure of the electrophoretic mobility of particles under an applied electric field of 3 v using the following equations: (μ_E (mobility) = v(velocity)/E(electric field); ξ (zeta potential) = 3 η(viscosity)* μE)/$2\varepsilon_r\varepsilon_0$. The electrophoretic mobility was measured using massively parallel phase analysis light scattering (MP-PALS), which collects independent and simultaneous measurements from 31 detector channels. The ξ potential in these studies is the electric potential at the boundary of the Debye length, which was calculated based on the Huckel model. The hydrodynamic radii of the samples were measured simultaneously using the Mobius® with a QELS module for measurement of dynamic light scattering. Dynamics® software was used to analyze and processes data from the MP-PALS and dynamic light scattering into size distributions, ξ potential and effective and net charge.

Brownian motion results in light intensities, which fluctuate in time, small particles fluctuate faster than larger molecules. The software uses autocorrelation functions to analyze decay times of molecules. The exponential decay rate of the autocorrelation function is proportional to the translational diffusion coefficient of molecules in solution and therefore the size of the molecules. Mono-modal and multi-modal complexes were fit to single or a set of (regularization) exponentials of diffusion constants, respectively. Regularization analysis resolved distinct size populations into histogram peaks, which include the radius and width. The hydrodynamic radii of protamine-heparin complexes were analyzed using both methods of analysis and fit primarily to a single exponential or mono-modal size distribution with > 88% of intensity defined in a single peak. Therefore, Rh single fit was similar to Rh regularization. A single exponential equation of diffusion constants was used to calculate the radii shown in Table 3.

Table 3
Radii and ξ potential measurements from model heparin oligosaccharide-protamine complexes.

Heparin	Radius		ξ potential (mV)	
	3 min	60 min	3 min	60 min
Heparin	49.0	51.1	29.8	29.6
Enoxaparin	48.4	47.8	29.7	31.8
NS 10-mer**	87.9	284.5	37.3	35.7
NS6S 10-mer**	69.8	135.0	38.6	43.6
NS2S 10-mer**	82.6	234.2	40.5	43.9
NS6S2S 10-mer**	63.3	121.8	41.1	45.7
NS 12-mer**	95.3	265.1	36.9	38.9
NS6S 12-mer*	52.8	66.4	39.0	38.8
NS2S 12-mer**	95.7	261.7	45.1	49.1
NS6S2S 12-mer	48.8	51.0	45.1	43.5
NS 14-mer*	76.9	178.9	33.0	33.1
NS6S 14-mer	55.2	55.6	34.4	38.7
NS2S 14-mer*	52.5	71.9	26.8	31.4
NS6S2S 14-mer	44.1	43.0	23.1	21.1
NS 16-mer*	61.6	111.8	38.7	40.5
NS6S 16-mer	50.4	54.6	29.5	33.0
NS2S 16-mer	46.0	46.7	27.8	26.2
NS6S2S 16-mer	59.6	59.0	49.1	46.0
NS 18-mer*	56.1	73.7	25.4	30.4
NS6S 18-mer	51.3	50.2	36.3	30.7
NS2S 18-mer	51.7	51.8	34.6	33.5
NS6S2S 18-mer	59.1	59.8	44.4	43.3

* $t < 0.001$.
** $t < 0.0001$ 2 tailed-t test comparison of radii at 3 min versus 60 min.

2.5. Optical Density at 280_{nm}

Protamine, heparin, enoxaparin and the model heparin oligosaccharides were prepared as 10 mg/mL stocks in Hanks balanced salts buffer. Protamine was diluted to 200 μg/mL and 180 μL added to a 96-well Greiner UV plate. Twenty microliter of each heparin or synthetic analog diluted to a 20x concentration was added in duplicate to protamine. The plate was gently tapped to mix and absorbance read at 280 nm from 1 to120 min in BioTek Synergy II microplate reader. Background absorbance was obtained by measuring each concentration of heparin or protamine alone. Protamine, unfractionated heparin or enoxaparin did not have intrinsic absorption. The model heparin oligosaccharides had background absorbance at all concentrations tested, which were subtracted from the wells containing heparin plus protamine.

2.6. Anticoagulation Assays

Anti-IIa and anti-Xa assays were performed on Sysmex CA-1500 system (Siemens Healthcare, Deerfield, IL) with Kinetichrome test kits (Provision Kinetics, Arlington, WI). The assays were designed according to US Pharmacopeia (USP) test method using USP heparin assay standard. Briefly, standard solution was prepared at 0.3750 IU/mL with Tris-saline buffer (Tris 0.05 M, NaCl 0.175 M, EDTA 0.0075 M, 0.1% PEG-8000, pH 8.4). For anti-IIa testing, thrombin (40 IU) and antithrombin (2.5 IU) were reconstituted with 10.0 and 5.0 mL of tris-saline buffer, respectively. For anti-Xa testing, factor Xa (25 μg) and antithrombin (5.0 IU) were reconstituted with 10.0 and 5.0 mL of tris-saline buffer, respectively. Both IIa and Xa substrates were reconstituted with 5.0 mL of high purity water. Standard and samples were analyzed in duplicate with 6 dilutions. Heparin standard, enoxaparin and model heparin oligosaccharides were diluted from 10 mg/mL stocks by a factor of 6019, 1720 and 100 fold, respectively, for starting concentrations. The lowest detectable heparin concentration was approximately 0.062 IU/mL. Raw data were processed by plotting known concentrations as a function of the log of ΔOD. Linear regression analysis was used to obtain the slopes of the standard and samples. The anti-IIa and anti-Xa activities were obtained from the slope ratios of the standard and samples.

3. Results

3.1. Heparin-Protamine Complex Profiles in Analytical Models

Fig. 1 A shows the ability of unfractionated heparin, at a given protamine concentration, to reduce the ξ potential (lower ratios = excess heparin) of the protamine/heparin solution. The protamine/heparin mass (mg/mL) ratio that yielded net neutrality occurred at approximately 1.5. The hydrodynamic radii and OD_{280} were measured by dynamic light scattering and by changes in light absorption to measure size and formation of the complexes (Fig. 1B). With increasing heparin concentrations there were significant changes in radius and light scattering until the amount of heparin saturated or neutralized protamine. The changes were bell-shaped with very similar peaks occurring at an approximate protamine/heparin ratio of 1.4. The peak radius was approximately 50 nm while peak absorbance was 1.3 OD at OD_{280}.

The formation of protamine/heparin complexes as shown by ξ potential, radius and OD_{280} occurred within 1–2 min after addition of heparin (Fig. 1C; ratio 1.7). Measurements of the radius and zeta potentials were very stable from 2 to 90 min, independent upon protamine/heparin ratio used for analysis. In contrast, complex turbidity as measured by OD_{280} values peaked and decreased steadily over time. In the OD_{280} model, samples were unfiltered and higher concentrations of reactants were used (i.e., 0.2 mg/mL (OD_{280}) versus 0.1 mg/mL (radius) protamine). The decrease in absorbance likely reflects the settling of large particulates beyond the 300–700 kDa size range. While the OD_{280} model is useful for rapid stoichiometric screening, this measurement lacks the sensitivity and accuracy observed in the hydrodynamic radii measurements.

3.2. Characterization of 12-mer-Protamine Complexes in Analytical Models

Table 1 and Fig. 2 show the size, number of sulfate groups, with or without IdoA2S residue, MW and structures of a set of model heparin oligosaccharides bearing varying length sequences of repeat disaccharides comprised of types of disaccharides found in heparin. These model heparin oligosaccharides have sizes from dodecasaccharides (10-mers) to octadecasaccharides (18-mers). Under each size group, five members are included to cover different sulfation types with or without the IdoA2S residue from heparin. Because the sulfo groups carry a negative charge under neutral pH, oligosaccharides having more sulfo groups display higher levels of negative charge under the experimental conditions in this study. These oligosaccharides offer a unique collection of model compounds to study the contribution of sizes, negative charges and the presence of IdoA2S residues to the binding to protamine.

Kinetic profiles of heparin, enoxaparin and/or 12-mer-protamine complex radii were evaluated using a protamine/heparin ratio of 1.7 (Fig. 3). Preliminary experiments showed optimal ratios for peak radii from all heparin samples between 1.7 and 1.3. The ratio curves were relatively flat and not associated with the 12-mer charge, therefore kinetic studies and direct comparisons of radii were made from multiple samples (2–5 measured 5–10 times), using a ratio of 1.7.

The kinetic stability of radii measurements of protamine-heparin oligosaccharide complexes, using the 12-mer set (structures shown in Fig. 2), was dependent upon the sulfation levels of the oligosaccharides (Fig. 3A). Protamine alone or in complex with heparin, enoxaparin, NS6S 12-mer (with 12 sulfo groups) and NS6S2S 12-mer (with 15 sulfo groups) had relatively stable radii from 3 to 60 min (Fig. 3A). Conversely, the radii of the NS 12-mer (with six sulfo groups) or NS2S 12-mer (with 9 sulfo groups) protamine complexes increased significantly and steadily over time (Fig. 3A). In a separate set of experiments, direct comparisons of complex radii at 3 min compared to 60 min showed significant differences ($t < 0.001–0.0001$) between the NS6S 12-mer, NS2S 12-mer and NS 12-mer radii (Table 2). Kinetically unstable radii, as measured by increasing radii, from the NS 12-mer and NS2S 12-mer protamine complexes were also observed with protamine/heparin ratios above (i.e., 2.5) and below (i.e., 1) the tested radii ratio of 1.7, suggesting that unstable complexes form in the presence of excess reactants.

Protamine complexes with the di-sulfated (NS6S and NS2S) and tri-sulfated (NS6S2S) 12-mers with the number of sulfo groups from 9 to 15 had similar peak ratios (1.35) in the OD_{280} model as heparin, whereas the single sulfated form (NS), or NS 12-mer with 6 sulfo groups, had a comparable ratio (0.9) to enoxaparin. Overall, peak OD values from 12-mer-protamine complexes were similar to each other but significantly less than OD values observed for heparin or enoxaparin-protamine complexes (Table 2). Given the decrease in OD values for all the complexes overtime and the OD interference from the pNP group in 12-mers, values from the OD_{280} model were deemed less informative about the size of complexes formed compared with the other models.

In contrast to the radii profiles, ξ potentials of protamine and heparin complexes were relatively stable from 3 to 60 min, independent of the ratio of reactants, for all the 12-mers, enoxaparin and unfractionated heparin. Fig. 3B shows the increase in ξ potential with decreasing heparin concentrations (higher ratios) for all the different 12-mers, regardless of sulfation level. The protamine/heparin ratios where ξ potential values were neutral (x-axis intercept) ranged from 1.44 (heparin) to 0.95 (NS 12-mer) as shown in Table 2. The rank order of heparin forms (from high to lower concentrations) to attain neutral charged complexes with a fixed amount of protamine was NS 12-mer > NS6S 12-mer ~ NS2S 12-mer > NS6S2S 12-mer ~ enoxaparin > heparin (Fig. 3B, Table 2).

These data showed the association between the number of sulfo groups, which alters the level of negative charge, and the capacity of each standard to reach complex neutralization. Protamine complexes with the di-sulfated 12-mers, NS2S 12-mer and NS6S 12-mer, have similar x-axis intercepts (1.15 versus 1.09, respectively), indicating that that the location of the charge on an IdoA residue or on a GlcNS residue was not a critical parameter for deter-

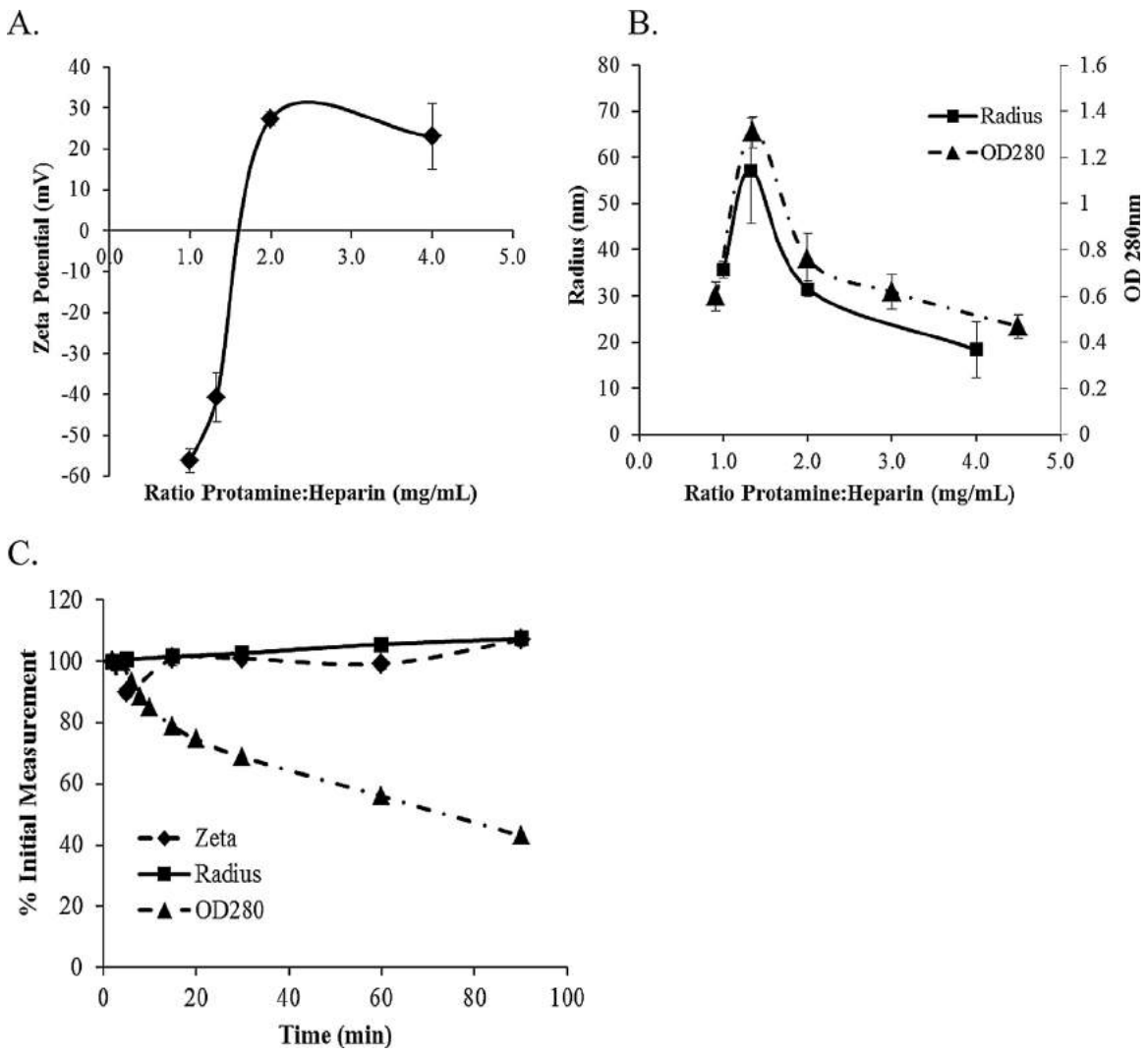

Fig. 1. Representative plots from analytical measurements of heparin-protamine complexes. Protamine concentrations ranged from 0.1 to 0.2 mg/mL with heparin concentrations ranging from 0.025 to 0.1 mg/mL. Ratios (A, B) are protamine/heparin concentrations, expressed on the x-axis. Kinetic plots (C) are from a protamine/heparin ratio of 1.7 (ξ potential and radius) and 1.4 (OD_{280}) measured from 2 to 90 min. Zeta potentials (A) were measured 15 min after complex formation and (B) hydrodynamic radii (squares) and OD_{280nm} (triangles) were measured 60 min after complex formation. Zeta potentials and radius measurements were averaged from 3 to 4 independent samples with 5–10 readings/sample. OD_{280} measurements were averaged from three experiments (B) or a representative experiment repeated twice (C). Data represent the mean ± standard error of the mean.

mining surface charge even though the charge was important for radii measurements. The summarized analytical data in Table 2 showed that heparin charge and/or structure played specific roles depending upon the test. Charge was critical for ξ potential whereas the presence of IdoA2S residues was more important in the radii model.

3.3. *Mechanistic Studies of Radii and ξ Potential Measurements using a Broader set of Model Heparin Oligosaccharides*

Table 3 summarizes the comparison of radii determined at 3 and 60 min from a larger set of model heparin oligosaccharides using a protamine-heparin ratio of 1.7. Interestingly, all the 10-mers, regardless of charge, have statistically significant ($t < 0.0001$) increases in protamine complex radii from 3 min (range 63.3–87.9 nm) to 60 min (range 135–285 nm). The rank order of increasing size was NS (radius of 285 nm) > NS2S (234 nm) > NS6S (135 nm) > NS6S2S (122 nm). By contrast, radii of the 18-mer-protamine complexes showed stable kinetic profiles, with the exception of the NS 18-mer, similar to those of heparin-protamine (Fig. 3A). In the 14 and 16-mers, only the radii of the NS 14-mer, NS2S 14-mer and NS 16-mer protamine complexes increased significantly with time and to a much lesser extent than the radii change observed with the 10 and 12-mers. The strong correlation between times dependent increases in the NS (N-sulfo oligosaccharide)-protamine complexes with the size ranging from 10 to 18-mer is shown in Fig. 4. NS, NS6S and NS2S protamine complex radii showed increased stability (less change in radii) as the length of the heparin chain increased from 10 to 18-mer (Table 3).

The increase in size of the NS and NS2S-protamine complexes could reflect increasing polydispersity. The level of polydispersity of the 12-mer peaks at 60 min were slightly higher (range 32–48%) than the levels at 3 min (range 28–33%) ($p = 0.025$), however this trend was also observed with heparin (39% at 5 min and 44% at 60 min). Of note, only single peaks were observed for all the oligosaccharide protamine complexes at 60 min, which are best described as mono-modal distributions that were polydisperse. These data suggest that aggregation of complexes observed with the NS and NS2S groups was occurring as a single peak containing the majority of complex mass and was not attributed to a

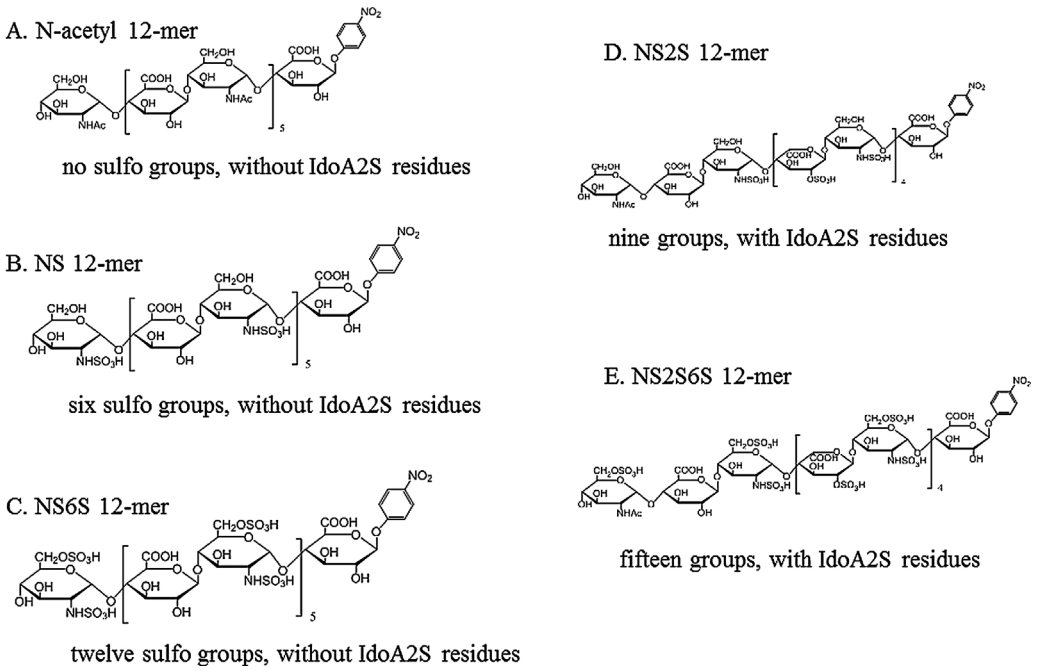

Fig. 2. Structures of different 12-mers used in this study. A) *N*-acetyl 12-mer; B) NS 12-mer; C) NS6S 12-mer; D) NS2S 12-mer and D) NS6S2S 12-mer. Structural feature for each member is described underneath of each structure.

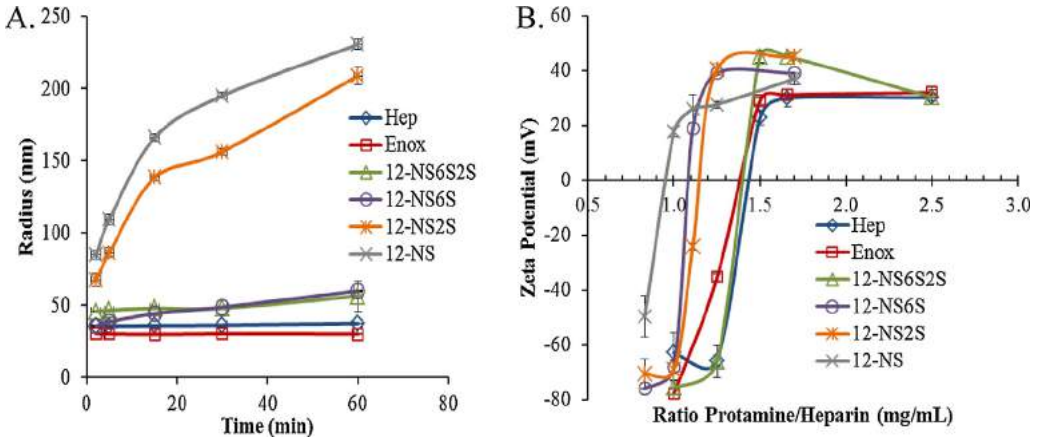

Fig. 3. Representative kinetic profiles of the averaged radius (A) and ratio profiles of ξ potentials (B) of oligosaccharide (12-mer)-protamine complexes. For radii measurements, the protamine-heparin ratio was 1.7 with protamine concentration of 0.1 mg/mL and heparin concentration of 0.06 mg/mL. Radii were measured 2–60 min following complex formation from 2 to3 samples over time. For ξ potentials, heparin, enoxaparin and 12-mers (0.04–0.2 mg/mL) were added to a fixed amount of protamine (0.1 mg/mL) and ξ potential measured 3 min after heparin addition from 2 to 3 samples with 5–10 measurements/sample. Data represent the mean ± standard deviation.

poly-modal or wider distribution of complex species or protamine aggregates with different masses.

Zeta ξ potentials from protamine complexes were evaluated using the larger set of model heparin oligosaccharides to discern the impact of charge and structure across chain lengths from 10 to 18 oligosaccharides long. Zeta potentials from all the complexes were stable over time (Table 3). The tri-sulfated oligosaccharides (NS6S2S 12–18-mer) protamine complexes had overlapping ξ potential profiles with unfractionated heparin independent of the chain length (Fig. 5A). By contrast, the di-sulfated oligosaccharides, NS6S oligosaccharides, required more heparin (lower ratios) to neutralize protamine at every size ranging from 12 to 18-mer, compared with unfractionated heparin (Fig. 5B). Complexes formed using the NS2S and NS oligosaccharides also had overlapping ξ potential profiles within each group, which were distinct from the profiles of heparin-protamine complexes (data not shown). The range of x-axis intercepts for the NS6S2S, NS6S, NS2S and NS groups were 1.36–1.40, 1.1–1.15, 1.15–1.16 and 0.93–0.95, respectively (Table 4).

Table 4
Summary of anticoagulant activities.

Potency IU/mg		
Samples	Anti-IIa	Anti-Xa
Heparin USP	225.7	226.4
Enoxaparin	24.7	68.5
18-NS6S2S	<LOD	2.31

3.4. Anticoagulant Activities of Heparin, Enoxaparin and Synthetic Heparins

Heparin exerts an anticoagulant effect as a cofactor with the inhibitor antithrombin (AT) through an AT binding site. LMWHs

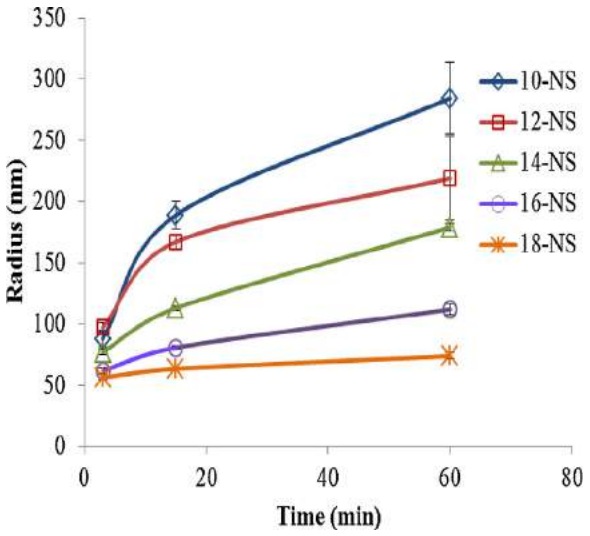

Fig. 4. Representative kinetic profiles of the averaged radii from NS 12-mer to NS 18-mer-oligosaccharide protamine complexes. Model heparin oligosaccharides (0.06 mg/mL) were added to a fixed amount of protamine (0.1 mg/mL) and radii measured following 60 min. The data represent the average ± standard deviation of 2–3 samples measured 5–10 times.

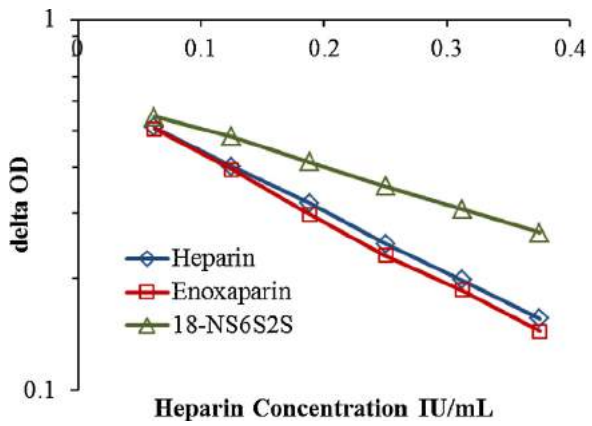

Fig. 6. Anti-factor Xa activity of heparin (diamonds), enoxaparin (squares) and NS6S2S 18-mer (triangles). Factor Xa (2.5 μg/mL), antithrombin (1.0 IU/mL) and heparin standard (0.375 IU/mL) were reconstituted in Tris-saline buffer. Standard and samples were analyzed in duplicate with 6 dilutions. Heparin standard, enoxaparin and synthetic heparins were diluted from 10 mg/mL stocks by a factor of 6019, 1720 and 100 fold, respectively, for starting concentrations. The raw data were processed by plotting known concentrations against the log of the ΔOD. Anti-Xa activities were obtained from the slope ratios of the standard and samples.

inactivate both factor Xa and to a lesser extent thrombin (factor IIa) when complexed with AT. Fig. 6 shows an overlay of concentration versus log delta OD values for factor Xa for heparin, enoxaparin and NS6S2S 18-mer. Heparin and enoxaparin have overlapping concentration anti-factor Xa curves, in contrast to the curve for NS6S2S 18-mer. On an IU/mg basis, the potency for NS6S2S 18-mer (~2 IU/mg) is about 30 fold and 100 fold less than enoxaparin (similar MW) and heparin, respectively. As expected, enoxaparin has about a third less activity against thrombin (24.7 IU/mg) compared with factor-Xa (68.5 IU/mg) and is about 3.3 fold less potent than heparin (weight basis) in the factor-Xa assay. The NS6S2S 18-mer was the only oligosaccharide with activity in the anti-factor Xa assay and none of the model heparin oligosaccharides showed measurable activity in the anti-factor IIa assay (including the 18-mer) when tested at concentrations 60 fold higher than that required for heparin. These data show the requirement of sulfation and chain length for anticoagulant activity in this set of model heparin oligosaccharides.

4. Discussion

Despite being the major therapeutic drug for prevention and treatment of thrombosis, heparin has a number of disadvantages including being a complex mixture and the occurrence of heparin-induced thrombocytopenia (HIT) [1,4]. Heparin can bind positively charged proteins including PF4 or protamine to form large antigenic complexes that upon antibody binding may cause serious immune reactions including thrombocytopenia and thrombosis [1,4,13]. In this article, potential mechanisms for heparin-protamine complex formation were elucidated using a set of well-defined homogeneous model heparin oligosaccharides of heparin sequence ranging from 10 to 18 monosaccharides in length [18]. The contributions of size and sulfation state from the oligosaccharides to the binding to protamine were shown in models of ξ potential and hydrodynamic

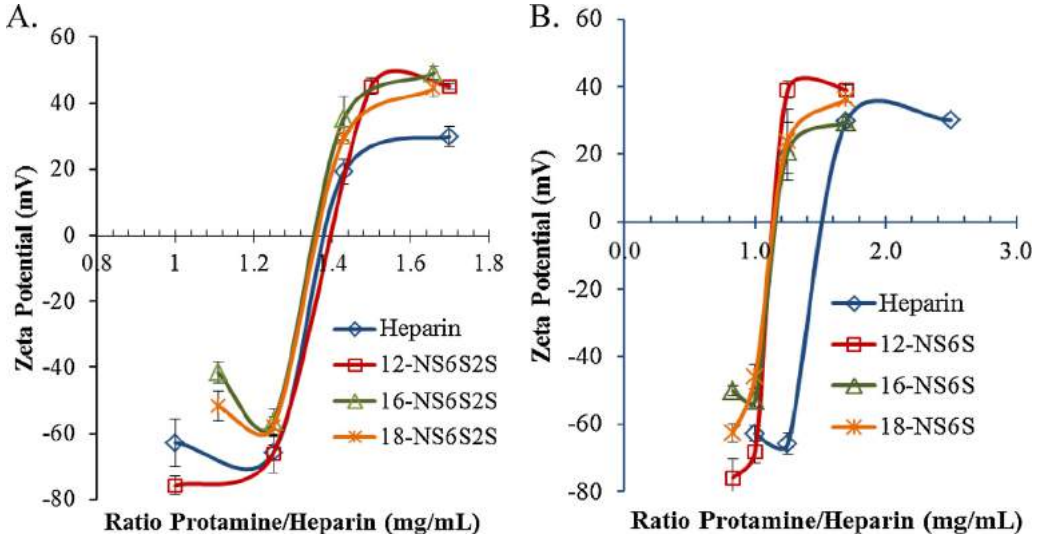

Fig. 5. Representative plots of ξ potentials of heparin (A, NS6S2S oligosaccharides; B, NS6S oligosaccharides)-protamine complexes. Unfractionated heparin and oligosaccharides (0.04–0.15 mg/mL) were added to a fixed amount of protamine (0.1 mg/mL) and ξ potential measured 3 min after heparin addition. The data represent the average ± standard deviation of 2–3 samples measured 5–10 times.

radii. To our knowledge, this is the first time a set of homogeneous oligosaccharides ranging in size from 10 to 18-mer and in sulfation from 0 to 2.8 sulfo groups/disaccharide unit has been used to study heparin complex binding with protamine.

Protamine sulfate is a cationic polypeptide inhibitor of heparin and is used clinically to neutralize both heparin sodium as well as LMWH after cardiopulmonary bypass surgery (CPB) and haemodialysis [4,19,20]. Neutralization is based on complex formation of the positively charged amino groups of protamine with the negatively charged sulfate groups of heparin. At least two arginine clusters within the protamine molecule are required to achieve binding and neutralization of the anticoagulant activity of heparin [21]. Some studies indicate that the degree of neutralization, as measured by heparin anti-Xa activity, correlates with molecular weight, implying that large heparin polysaccharide chains have higher affinity for protamine compared with short LMWH oligosaccharide chains [9,22]. Other studies suggest the degree of sulfation is the most important factor [23] for determining the binding affinity and thus efficacy of protamine.

Here, the only model heparin oligosaccharide with detectable anti-Xa activity was the tri-sulfated 18-mer, or NS6S2S 18-mer, which was 30-fold less potent than enoxaparin. In a recent report, a super sulfated 12-mer (S12-mer; containing 17 sulfate groups), engineered with 3-*O*-sulfation at sites to preserve anti-factor Xa activity, showed anti-factor Xa potency with an IC_{50} of 99.7 nM compared with 147 nM for enoxaparin [10]. In addition, the S12-mer showed similar in vivo activity against thrombosis and fibrin formation as enoxaparin. The control 12-mer (similar to NS6S2S 12-mer), had no activity against thrombin or factor Xa. Therefore, our data suggest that the additional length of the tri-sulfated 18-mer can partially compensate for the loss of 3-*O*-sulfation required for anticoagulant activity by S12-mer. Differences in the anticoagulant activities between the studies most likely reflect the different forms of the synthetic heparins and requirement of an anti-thrombin binding site for full anti-factor Xa activity.

Recently, studies have shown that protamine undergoes conformational changes, similar to PF4 after binding to heparin, and that multi-molecular heparin-protamine complexes induce IgG antibodies in about 25% of patients after cardiac surgery [2,24]. Anti-protamine-heparin antibodies can activate platelets and cause postoperative complications such as arterial occlusions, delay in recovery of platelet count and, in rare cases, thrombocytopenia [2,25]. Chudasama et al., showed that protamine-heparin complexes are immunogenic over a certain range of heparin concentrations and that the immune response was attenuated when either component was in excess [11]. Using techniques to measure changes in ξ potential and absorbance, Chudasama et al., demonstrated component ratio dependence for optimal binding or neutralization. Optimal ratios observed in the analytical models were also optimal for dendritic cell activation and production of specific anti-heparin-protamine antibodies in a murine model.

The properties observed for heparin-protamine complexes (e.g., ξ potentials, OD_{280} profile and radius) in this work were similar to those reported in the literature where transition from positive to negative values and peak optical densities and radii occurred above a protamine to heparin ratio of 1 (based on mass mg/mL) [7,11,15]. For example, Maurer et al., showed comparable kinetic profiles of light scattering at 45° for heparinized plasma samples (3–24 IU/mL heparin) after protamine addition [15]. Peak intensities were observed after 5 min and were relatively stable over at least 20 min [15]. Published radii and nanoscale particle size for protamine complexes formed with heparin or LMWH (Clexane) were approximately 30 nm and 60 nm using sedimentation velocity and atomic force microscopy and 20–100 nm using light scattering at 45° [15], consistent with the radii [~35–50 nm] observed here with heparin and enoxaparin using dynamic light scattering measurements.

The minimum molecular size of heparin required for complete neutralization of activity by protamine has been suggested to be at least 18 saccharide units [9,23]. Liu and coworkers previously demonstrated that a heparin oligosaccharide having anti-Xa activity with 12 saccharide units could be completely neutralized with protamine [17]. The synthetic pentasaccharide fondaparinux has a molecular weight of 1728 and is highly sulfated, however fondaparinux is resistant to neutralization by protamine. Interestingly, fondaparinux does form complexes with PF4 with about half the radius of heparin-PF4 complexes [26]. Using a diverse set of LMWH and monodisperse oligosaccharide fractions, Schroeder's group proposed that neutralization of LMWH activity was strongly dependent on molecular weight, but that other structural factors were also at play [9]. Here, the kinetic stability of radii was found to be highly dependent upon chain length. Thus, radii from protamine complexes with 10-mers increased over time, whereas radii from protamine complexes with 18-mers (with exception of NS 18-mer) were stable over 60 min, similar to that observed with either heparin or enoxaparin complexes with protamine. Within the 12–16-mers, complex stability was dependent upon the degree of sulfation.

Interestingly, in the ξ potential model, chain length did not appear to play a role within a particular model heparin oligosaccharide. For example, NS6S (10–18-mer), NS2S (10–18-mer) and NS (10–18-mer) complexes with protamine had overlapping x-axis intercepts at ratios less than that observed with heparin-protamine. The complexes with tri-sulfated oligosaccharides (NS6S2S 12–18-mer) had ξ potential profiles very similar to heparin. Given the increase in surface charge with heparin chain length, why the zeta potential profiles of complexes with the di-sulfated and mono-sulfated oligosaccharides did not show shifts toward the profile of heparin was not clear.

The glucuronic or iduronic acid (GlcA/IdoA) units of heparin can be sulfated at several positions (NS2S), and the glucosamine (GlcN) residue can be unsubstituted (NH_2), acetylated (N-acetyl) or sulfated (NS). The degree and location of sulfation are critical for heparin anticoagulant activity and for neutralization by protamine. For example, *O*-desulfated heparin is a partially desulfated heparin (2-sulfate, 3,6-disulfate) and has been shown to possess very low binding affinity for anti-thrombin and has low anticoagulant activities [27]. Heparin, however, has the capacity to interfere with heparin induced structural changes of protamine as well as platelet activation by heparin-protamine complexes [28], suggesting that other sulfate groups are sufficient for heparin to compete with heparin for binding to protamine or for antibody binding. In contrast, treatment of heparin with Sulf-2, a 6-*O*-endosulfatase, which removes the 6-*O*-sulfation from glucosamine, has been shown to preserve binding to antithrombin while reducing binding of heparin to PF4 by 10–20 fold [29]. Thus, the inability of protamine to neutralize the activity of a sub-fraction of LMWH has been attributed to decreased sulfate (*O* and *N*) content [23]. As such, the variable sulfate charge densities in different commercially available LMWH correlate with their ability to be neutralized by protamine [23].

Here, the location and degree of sulfation is shown to influence protamine complex stability and radii. Protamine complexes with NS6S2S 12-mer to NS6S2S 18-mer have similar radii and stability as heparin-protamine complexes, whereas NS 10-mer to NS 18-mer complexes (lacking 2 and 6-O-sulfation) all have radii that increase over time and probably reflect weaker binding to protamine. Interestingly, a distinct difference in the size and stability of complex radii formed by the di-sulfated NS2S 10-mer to NS2S 14-mer versus the NS6S 10-mer and NS6S 14-mer was observed but not with the 16–18-mer counterparts. These data illustrate that protamine

binding can be impacted by both sulfation location and size of the sulfation types (i.e., longer chain lengths can compensate for differences in sulfation location). Interestingly, the sulfation location did not impact the x-axis ξ potential intercepts, whereas the degree of sulfation clearly impacted the amount of heparin required to neutralize protamine.

Overall, the binding stability of model heparin oligosaccharides to protamine is dependent upon size, sulfation degree and location. Similar conclusions have been made in the literature with respect to protamine neutralization of LMWH [9,23]. Here, our observations are consistent with a model where when the binding affinity of the heparin chain due to ionic interaction with protamine reaches a certain threshold the complex remains stable over time. Thus, the shorter less sulfated chains are binding but partially or completely dissociating in a dynamic equilibrium that results in an increase in the complex size with time.

In summary, data from the ξ potential and hydrodynamic radii models, using this diversified set of model heparin oligosaccharides, showed the robustness of these measurement techniques and their utility to distinguish analytical differences between protamine complexes formed with heparin sequences. The oligosaccharides used in this study are in the size range of low-molecular weight heparin, much closer to the properties of heparin than short oligosaccharides such as pentasaccharides or hexasaccharides. Of course, these homogeneous model heparin oligosaccharides may not fully represent the properties of heterogeneous heparin polysaccharides. Nevertheless, the availability of a broad set of model heparin oligosaccharides provides insights into the formation of heparin/protamine complexes. Understanding the mechanism(s) of heparin complex formation with protamine and/or PF4 opens the door for the development of safer heparin therapeutics. Ultimately, comparisons can be made between complexes formed with protamine or PF4 and model heparin oligosaccharides to establish links between the charge and/or size of heparin and the formation of large immunogenic complexes.

FDA Disclaimer

The findings and conclusions in this article have not been formally disseminated by the Food and Drug Administration and should not be construed to represent any Agency determination or policy.

Acknowledgments

This work was supported by an FDA Critical Path grant to Cynthia Sommers and FDA funding to Drs. Liu and Linhardt.

References

[1] T.E. Warkentin, A. Greinacher, Heparin-induced thrombocytopenia and cardiac surgery, Ann. Thorac. Surg. 76 (2003) 2121–2131.
[2] T. Bakchoul, H. Zollner, J. Amiral, S. Panzer, S. Selleng, T. Kohlmann, S. Brandt, M. Delcea, T.E. Warkentin, U.J. Sachs, A. Greinacher, Anti-protamine-heparin antibodies: incidence, clinical relevance, and pathogenesis, Blood 121 (2013) 2821–2827.
[3] H. Schellekens, The immunogenicity of therapeutic proteins, Discov. Med. 9 (2010) 560–564.
[4] G.M. Arepally, T.L. Ortel, Clinical practice. Heparin-induced thrombocytopenia, N. Engl. J. Med. 355 (2006) 809–817.
[5] B. Mulloy, E. Gray, T.W. Barrowcliffe, Characterization of unfractionated heparin: comparison of materials from the last 50 years, Thromb. Haemost. 84 (2000) 1052–1056.
[6] A.M. Brustkern, L.F. Buhse, M. Nasr, A. Al-Hakim, D.A. Keire, Characterization of currently marketed heparin products: reversed-phase ion-pairing liquid chromatography mass spectrometry of heparin digests, Anal. Chem. 82 (2010) 9865–9870.
[7] C.D. Sommers, N. Montpas, A. Adam, D.A. Keire, Characterization of currently marketed heparin products: adverse event relevant bioassays, J. Pharm. Biomed. Anal. 67–68 (2012) 28–35.
[8] J.I. Weitz, Low-molecular-weight heparins, N. Engl. J. Med. 337 (1997) 688–698.
[9] M. Schroeder, J. Hogwood, E. Gray, B. Mulloy, A.M. Hackett, K.B. Johansen, Protamine neutralisation of low molecular weight heparins and their oligosaccharide components, Anal. Bioanal. Chem. 399 (2011) 763–771.
[10] M.F. Whelihan, B. Cooley, Y. Xu, R. Pawlinski, J. Liu, N.S. Key, In vitro and in vivo characterization of a reversible synthetic heparin analog, Thromb. Res. 138 (2016) 121–129.
[11] S.L. Chudasama, B. Espinasse, F. Hwang, R. Qi, M. Joglekar, G. Afonina, M.R. Wiesner, I.J. Welsby, T.L. Ortel, G.M. Arepally, Heparin modifies the immunogenicity of positively charged proteins, Blood 116 (2010) 6046–6053.
[12] G.M. Lee, I.J. Welsby, B. Phillips-Bute, T.L. Ortel, G.M. Arepally, High incidence of antibodies to protamine and protamine/heparin complexes in patients undergoing cardiopulmonary bypass, Blood 121 (2013) 2828–2835.
[13] A. Cuker, D.B. Cines, Protamine-induced thrombocytopenia? Blood 121 (2013) 2818–2819.
[14] S. Suvarna, B. Espinasse, R. Qi, R. Lubica, M. Poncz, D.B. Cines, M.R. Wiesner, G.M. Arepally, Determinants of PF4/heparin immunogenicity, Blood 110 (2007) 4253–4260.
[15] J. Maurer, S. Haselbach, O. Klein, D. Baykut, V. Vogel, W. Mantele, Analysis of the complex formation of heparin with protamine by light scattering and analytical ultracentrifugation: implications for blood coagulation management, J. Am. Chem. Soc. 133 (2011) 1134–1140.
[16] C.D. Sommers, H. Ye, R.E. Kolinski, M. Nasr, L.F. Buhse, A. Al-Hakim, D.A. Keire, Characterization of currently marketed heparin products: analysis of molecular weight and heparinase-I digest patterns, Anal. Bioanal. Chem. 401 (2011) 2445–2454.
[17] Y. Xu, C. Cai, K. Chandarajoti, P.H. Hsieh, L. Li, T.Q. Pham, E.M. Sparkenbaugh, J. Sheng, N.S. Key, R. Pawlinski, E.N. Harris, R.J. Linhardt, J. Liu, Homogeneous low-molecular-weight heparins with reversible anticoagulant activity, Nat. Chem. Biol. 10 (2014) 248–250.
[18] Y. Xu, S. Masuko, M. Takieddin, H. Xu, R. Liu, J. Jing, S.A. Mousa, R.J. Linhardt, J. Liu, Chemoenzymatic synthesis of homogeneous ultralow molecular weight heparins, Science 334 (2011) 498–501.
[19] K. Andrassy, Low molecular weight heparin and haemodialysis: neutralization by protaminchloride, Blood Coagul. Fibrin. 4 (Suppl 1) (1993) S39–S43.
[20] E. Gray, J. Hogwood, B. Mulloy, The anticoagulant and antithrombotic mechanisms of heparin, Handb. Exp. Pharmacol. (2012) 43–61.
[21] L.C. Chang, H.F. Lee, Z. Yang, V.C. Yang, Low molecular weight protamine (LMWP) as nontoxic heparin/low molecular weight heparin antidote (I): preparation and characterization, AAPS PharmSci. 3 (2001) E17.
[22] N. Ramamurthy, N. Baliga, T.W. Wakefield, P.C. Andrews, V.C. Yang, M.E. Meyerhoff, Determination of low-molecular-weight heparins and their binding to protamine and a protamine analog using polyion-sensitive membrane electrodes, Anal. Biochem. 266 (1999) 116–124.
[23] M.A. Crowther, L.R. Berry, P.T. Monagle, A.K. Chan, Mechanisms responsible for the failure of protamine to inactivate low-molecular-weight heparin, Br. J. Haematol. 116 (2002) 178–186.
[24] C. Pouplard, D. Leroux, J. Rollin, J. Amiral, M.A. May, Y. Gruel, Incidence of antibodies to protamine sulfate/heparin complexes incardiac surgery patients and impact on platelet activation and clinical outcome, Thromb. Haemost. 109 (2013) 1141–1147.
[25] S. Panzer, A. Schiferer, B. Steinlechner, L. Drouet, J. Amiral, Serological features of antibodies to protamine inducing thrombocytopenia and thrombosis, Clin. Chem. Lab. Med. 53 (2015) 249–255.
[26] A. Greinacher, S. Alban, M.A. Omer-Adam, W. Weitschies, T.E. Warkentin, Heparin-induced thrombocytopenia: a stoichiometry-based model to explain the differing immunogenicities of unfractionated heparin, low-molecular-weight heparin, and fondaparinux in different clinical settings, Thromb. Res. 122 (2008) 211–220.
[27] N.V. Rao, B. Argyle, X. Xu, P.R. Reynolds, J.M. Walenga, M. Prechel, G.D. Prestwich, R.B. MacArthur, B.B. Walters, J.R. Hoidal, T.P. Kennedy, Low anticoagulant heparin targets multiple sites of inflammation, suppresses heparin-induced thrombocytopenia, and inhibits interaction of RAGE with its ligands, American journal of physiology, Cell Physiol. 299 (2010) C97–C110.
[28] R. Jouni, H. Zollner, A. Khadour, J. Wesche, A. Grotevendt, S. Brandt, M. Delcea, K. Krauel, H. Schwertz, U.J. Sachs, A. Greinacher, T. Bakchoul, Partially desulfated heparin modulates the interaction between anti-protamine/heparin antibodies and platelets, Thromb. Haemost. 115 (2016) 324–332.
[29] E.H. Pempe, T.C. Burch, C.J. Law, J. Liu, Substrate specificity of 6-O-endosulfatase (Sulf-2) and its implications in synthesizing anticoagulant heparan sulfate, Glycobiology 22 (2012) 1353–1362.